



ORIGINAL PAPER

Fangming Lei · Zhengxi Chen · Chunlong Gu ·
Liansheng Ma · Yuanwen Gao

Propagation characteristics of Love waves in a layered piezomagnetic structure

Received: 1 February 2023 / Revised: 27 April 2023 / Accepted: 23 June 2023 / Published online: 20 July 2023
© The Author(s), under exclusive licence to Springer-Verlag GmbH Austria, part of Springer Nature 2023

Abstract Propagation characteristics of Love waves in a layered structure composed of a piezomagnetic layer attached to an elastic substrate exposed to a magnetic field and compressive stress are investigated theoretically in this article. The effective elastic, piezomagnetic and magnetic permeability constants of a piezomagnetic material can be affected by a magnetic field and compressive stress. The effects of magnetic field and compressive stress on the phase velocity, group velocity, mode shape, and magnetic potential of the Love wave are discussed in detail. It is found that the number of modes increases as the intensity of magnetic field increases while this tendency is reverse when applying compressive stress. As the intensity of magnetic field increases, the group velocity decreases but the magnitude of surface displacement of a piezomagnetic layer increases. The findings presented in this article are useful for improving the performance of surface acoustic wave (SAW) devices.

1 Introduction

SAW devices have been widely used in various electronic systems such as sensors, transducers, and delay lines. The advantage of these devices is the high sensitivity to external disturbances because the acoustic energy is concentrated near the surface within a few wavelengths [1]. Shear Horizontal (SH) waves, which include Love waves [2] and Bleustein–Gulyaev (BG) waves [3], appear usually as surface acoustic waves (SAWs) in signal-processing devices due to their high performance and simple particle motion [4]. To improve the performance of SAW devices, researchers devote themselves to search various methods to tune the propagation characteristics of SH waves in device structures.

Li [5] studied the optical effect on the velocity of BG waves and provided accurate formulas to evaluate the acousto-optic interaction due to the piezoelectricity of the substrate. Jin et al. [6] investigated the propagation of BG waves in layered piezoelectric structures. He found that the mechanical perturbation of the particles only takes place in the layer and does not penetrate into substrate when the piezoelectric, dielectric constants of the structures and the thickness of the layer satisfy a certain relationship. The advantage of this method is to increase the sensitivity and performance of the SAW devices. Li et al. [7, 8] studied systematically the

F. Lei (✉) · Y. Gao (✉)

Key Laboratory of Mechanics On Disaster and Environment in Western China, College of Civil Engineering and Mechanics, Lanzhou University, Lanzhou 730000, Gansu, People's Republic of China
e-mail: leifm@lut.edu.cn

Y. Gao
e-mail: ywgao@lzu.edu.cn

F. Lei · Z. Chen · C. Gu
School of Science, Lanzhou University of Technology, Lanzhou 730000, Gansu, People's Republic of China

L. Ma
School of Architecture and Art, Weifang University of Science and Technology, Weifang 262700, Shandong, People's Republic of China

propagation of BG waves in the layered piezoelectric structure and functionally graded transversely isotropic electro-magneto-elastic half-space. The effects of the imperfect interface between the layer and substrate as well as the effect of the gradient coefficient in the half-space on the dispersion relation of BG waves were discussed. They found that the electromechanical coupling factor of BG waves was substantially increased improved efficiently by the imperfect interface and the gradient coefficient.

Compared with the BG waves, there are multiple modes of the Love waves at a certain wavelength [9]. This makes the Love waves to have potential advantages in SAW devices. In general, Love waves do not exist in a homogeneous substrate. However, this existence condition is changed by designing the homogeneous substrate as a functionally graded infinite half-space [10–12]. This provided an efficient approach to improve the propagation characteristics of Love waves by tuning the gradient coefficient of the infinite half-space. By depositing the waveguide layers on a substrate, the mechanical energy of Love waves could be trapped in the layers [13] and the propagation characteristics could be tuned by additional parameters such as the thickness and material properties of the layer [14–19] and the interface conditions between the layer and substrate [20–22]. Besides the waveguide layer and interface conditions can affect the wave behavior, the propagation characteristics of SH waves can also be tuned by applying external bias fields such as an initial stress and electric field. These methods are easier to implement than changing the devices' structures. Su et al. [23] studied the propagation of Love waves in the layered piezoelectric media with inhomogeneous initial stresses by the method of transfer matrix. It was found that both the middle layer and the initial stress in layers affect the phase velocity, group velocity and electromechanical coupling coefficient obviously. Qian [24–26] and Du [27, 28] systematically investigated the effects of the homogeneous and inhomogeneous initial stress on the propagation of Love waves in layered piezoelectric/piezomagnetic structures. These studies demonstrated that the initial stress not only increases the magneto-electric coupling factor but also decreases the penetration depth of Love waves and stress concentration at the interface between the layer and substrate. Based on the theory of nonlinear continuum mechanics, theoretical analysis of BG surface acoustic wave propagation in a prestressed layered piezoelectric structure were described and an almost linear behavior of the relative change in phase velocity versus the initial stress was obtained [29]. The phase velocity of BG waves in piezoelectric semiconductors can be increased by applying the electric field along the propagation direction [30–34].

According to the authors' best knowledge, there are few researches on the propagation characteristics of SAWs affected by the external magnetic field. In order to improve the performance of SAW devices, the effects of the magnetic field and compressive stress on the propagation characteristics of Love waves in the layered piezomagnetic structure have been investigated in this article. The advantage of this method is that it is convenient to apply and the significant change of the wave characteristics can be achieved by applying a small external stimulation without changing the whole devices' structure.

2 Statement of the problem

A layered piezomagnetic structure is shown in Fig. 1. The elastic substrate occupies the region $x > 0$. A piezomagnetic layer with the thickness h is deposited on the surface of the substrate. Love waves propagate along the positive direction of the y -axis. The magnetic field and compressive stress are applied in the layer are along z direction. The nonlinear constitutive relation of the piezomagnetic material is [35]:

$$\begin{aligned} \varepsilon_{ij} &= \frac{1}{E} [(1 + \nu)\sigma_{ij} - \nu\sigma_{kk}\delta_{ij}] + \frac{\lambda_s}{M_s^2} \left[\frac{3}{2}M_iM_j - M_kM_k \left(\frac{1}{2}\delta_{ij} + \frac{\tilde{\sigma}_{ij}}{\sigma_s} \right) \right], \\ H_i &= \left\{ \frac{1}{k_r M} f^{-1} \left(\frac{M}{M_s} \right) \delta_{ij} - \frac{\lambda_s}{\mu_0 M_s^2} \left[\frac{2\tilde{\sigma}_{ij} - (I_\sigma^2 - 3\Pi_\sigma)\delta_{ij}}{\sigma_s} \right] \right\} M_j, \end{aligned} \quad (1)$$

where ε_{ij} and σ_{ij} are the strain and the stress tensors, E and ν are Young's modulus and Poisson's ratio, H_i is the magnetic field intensity along the i -axis direction, λ_s , M_s and σ_s are the saturation magnetostriction, magnetization and stress, respectively. $k_r = 3\chi_m/M_s$ is the relaxation factor, where χ_m is the susceptibility in the initial linear region. δ_{ij} is the Kronecker delta. $M = \sqrt{M_k M_k}$ denotes the magnitude of the magnetization vector \mathbf{M} . $I_\sigma^2 - 3\Pi_\sigma = 2\tilde{\sigma}_{ij}\tilde{\sigma}_{ij}/3$, where $\tilde{\sigma}_{ij} = 3\sigma_{ij}/2 - \sigma_{kk}\delta_{ij}/2$ is 3/2 times as much as the deviatoric stress of σ_{ij} . $f(x) = \coth(x) - 1/x$ is the Langevin function and $\mu_0 = 4\pi \times 10^{-7}$ H/m is the vacuum permeability.

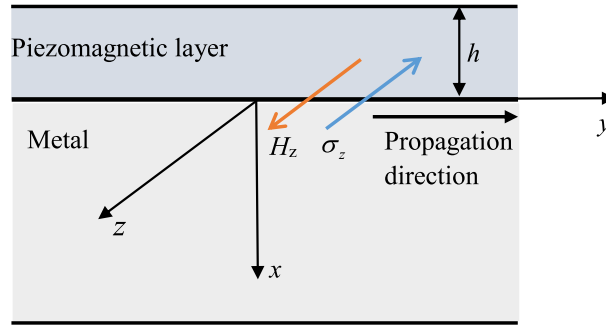


Fig. 1 Layered piezomagnetic structure

Using the engineering shear strain, the matrix forms of Eq. (1) shown in Appendix A can be put into the linear forms of the constitutive relations in the piezomagnetic material [36]:

$$\begin{aligned}\sigma_{ij} &= c_{ijkl}(\mathbf{H}, \boldsymbol{\sigma})\varepsilon_{kl} - q_{mij}(\mathbf{H}, \boldsymbol{\sigma})H_m, \\ B_n &= q_{nkl}(\mathbf{H}, \boldsymbol{\sigma})\varepsilon_{kl} + \mu_{nm}(\mathbf{H}, \boldsymbol{\sigma})H_m,\end{aligned}\quad (2)$$

where σ_{ij} and B_n are the components of the stress and magnetic induction, $c_{ijkl}(\mathbf{H}, \boldsymbol{\sigma})$, $q_{mij}(\mathbf{H}, \boldsymbol{\sigma})$ and $\mu_{nm}(\mathbf{H}, \boldsymbol{\sigma})$ are the effective elastic constants, piezomagnetic constants and magnetic permeability constants, respectively. \mathbf{H} and $\boldsymbol{\sigma}$ are applied magnetic field vector and stress vector. The expressions of these material constants are shown in Appendix B for brevity.

From Eq. (2) and parameters shown in Appendix B, the effective elastic constant c_{44} , piezomagnetic constant q_{15} and magnetic permeability constant μ_{11} are obtained:

$$\begin{aligned}c_{44} &= (S_{44})^{-1} = \left(\frac{\partial \gamma_{yz}}{\partial \tau_{yz}} \right)^{-1} = \left(\frac{1}{G} - \frac{3\lambda_s M_z^2}{\sigma_s M_s^2} + \frac{9k_r \lambda_s^2 \frac{M_z^2}{M_s^2}}{3\mu_0 M_s - k_r \lambda_s \left(2\tilde{\sigma}_y - \frac{I_\sigma^2 - 3\Pi_\sigma}{\sigma_s} \right)} \right)^{-1} \\ &= \frac{G\sigma_s M_s^2 (3\mu_0 M_s + k_r \lambda_s \sigma_t)}{\sigma_s M_s^2 (3\mu_0 M_s + k_r \lambda_s \sigma_t) - 3G\lambda_s M_z^2 (3\mu_0 M_s + k_r \lambda_s \sigma_t) + 9Gk_r \lambda_s \sigma_s M_s^2} \\ q_{15} &= d_{51} \cdot (S_{55})^{-1} = \frac{\partial \gamma_{zx}}{\partial H_x} \cdot \left(\frac{\partial \gamma_{zx}}{\partial \tau_{zx}} \right)^{-1} \\ &= \frac{3k_r \mu_0 \lambda_s M_z}{3\mu_0 M_s - k_r \lambda_s \left(2\tilde{\sigma}_x - \frac{I_\sigma^2 - 3\Pi_\sigma}{\sigma_s} \right)} \cdot \left(\frac{1}{G} - \frac{3\lambda_s M_z^2}{\sigma_s M_s^2} + \frac{9k_r \lambda_s^2 \frac{M_z^2}{M_s^2}}{3\mu_0 M_s - k_r \lambda_s \left(2\tilde{\sigma}_x - \frac{I_\sigma^2 - 3\Pi_\sigma}{\sigma_s} \right)} \right)^{-1} \\ &= \frac{3Gk_r \mu_0 \lambda_s \sigma_s M_z M_s^2}{\sigma_s M_s^2 (3\mu_0 M_s + k_r \lambda_s \sigma_t) - 3G\lambda_s M_z^2 (3\mu_0 M_s + k_r \lambda_s \sigma_t) + 9Gk_r \lambda_s \sigma_s M_s^2} \\ \mu_{11} &= \bar{\mu}_{11} - d_{51} \cdot (S_{55})^{-1} \cdot d_{51} = \frac{\partial B_x}{\partial H_x} - \frac{\partial \gamma_{zx}}{\partial H_x} \cdot \left(\frac{\partial \gamma_{zx}}{\partial \tau_{zx}} \right)^{-1} \cdot \frac{\partial \gamma_{zx}}{\partial H_x} \\ &= \mu_0 + \frac{k_r \mu_0^2 \lambda_s M_z}{3\mu_0 M_s - k_r \lambda_s \left(2\tilde{\sigma}_x - \frac{I_\sigma^2 - 3\Pi_\sigma}{\sigma_s} \right)} - \frac{\partial \gamma_{zx}}{\partial H_x} \cdot \left(\frac{\partial \gamma_{zx}}{\partial \tau_{zx}} \right)^{-1} \cdot \frac{\partial \gamma_{zx}}{\partial H_x} \\ &= \mu_0 + \frac{k_r \mu_0^2 M_s^2}{3\mu_0 M_s + k_r \lambda_s \sigma_t} \\ &\quad - \frac{9Gk_r^2 \mu_0^2 \lambda_s^2 \sigma_s M_z^2 M_s^2}{\sigma_s M_s^2 (3\mu_0 M_s + k_r \lambda_s \sigma_t)^2 - 3G\lambda_s M_z^2 (3\mu_0 M_s + k_r \lambda_s \sigma_t)^2 + 9Gk_r \lambda_s \sigma_s M_s^2 (3\mu_0 M_s + k_r \lambda_s \sigma_t)}\end{aligned}\quad (3)$$

where M_z is the magnetization along z-axis, $\tilde{\sigma}_x = -\sigma_z/2$, $\tilde{\sigma}_y = -\sigma_z/2$, $\tilde{\sigma}_z = \sigma_z$, and $\sigma_t = -(\sigma_z + \sigma_z^2/\sigma_s)$.

For Love waves propagation in the proposed structure shown in Fig. 1, the mechanical displacement components and magnetic potential are described as follows

$$u = v = 0, \quad w = w(x, y, t), \quad \varphi = \varphi(x, y, t), \quad (4)$$

where u , v , and w are the displacement components of Love waves along the x -axis, y -axis, and z -axis, respectively, and φ is the magnetic potential. Because the matrix forms of the effective material constants in the piezomagnetic material are the same as those in [36, 37], the governing equations of Love waves can be expressed as [37]:

$$\begin{aligned} c_{44}\nabla^2 w + q_{15}\nabla^2 \varphi &= \rho \ddot{w}, \\ q_{15}\nabla^2 w - \mu_{11}\nabla^2 \varphi &= 0, \end{aligned} \quad (5)$$

where c_{44} , q_{15} and μ_{11} are the elastic, piezomagnetic and magnetic permeability constants, respectively, ρ is the mass density, $\nabla^2 = \partial^2 / \partial x^2 + \partial^2 / \partial y^2$ is the two-dimensional Laplacian operator, and the dot refers to time differentiation. Following the Ref. [3], Eq. (5) can be written as the following form

$$\begin{aligned} \nabla^2 w - \left(1/c_p^2\right) \ddot{w} &= 0, \\ \nabla^2 [\varphi - (q_{15}/\mu_{11})w] &= 0, \end{aligned} \quad (6)$$

where $c_p = [(c_{44} + q_{15}^2/\mu_{11})/\rho]^{1/2}$ is the bulk shear wave speed in the piezomagnetic material.

For a metal substrate, let w' denote the mechanical displacement in the z direction. The governing equation for w' is [38]

$$\nabla^2 w' - (1/c_m^2) \ddot{w}' = 0, \quad (7)$$

where $c_m = (c'_{44}/\rho')^{1/2}$ is the bulk shear wave speed in the metal material, with c'_{44} and ρ' representing the shear modulus and mass density, respectively.

The wave propagation problem specified by Eqs. (6) and (7) should satisfy the following boundary and continuity conditions:

Mechanical boundary condition:

$$\sigma_{xz} = 0 \quad \text{at } x = -h; \quad (8a)$$

Magnetic closed boundary condition:

$$B_x = 0 \quad \text{at } x = -h; \quad (8b)$$

The continuity conditions at the interface between the layer and substrate at $x = 0$

$$w = w', \quad \sigma_{xz} = \sigma'_{xz}, \quad \varphi = 0, \quad (8c)$$

The attenuation condition

$$w' \rightarrow 0 \quad \text{as } x \rightarrow +\infty. \quad (8d)$$

3 Solution of the problem

Based on the earlier researches [38, 39], the solutions of Love waves propagation in the piezomagnetic layer and metal substrate can be expressed as:

$$\begin{aligned} w(x, y, t) &= (A_1 e^{-bkx} + A_2 e^{bkx}) \exp[ik(y - ct)], \\ \varphi(x, y, t) &= \left[A_3 e^{-kx} + A_4 e^{kx} + \frac{q_{15}}{\mu_{11}} (A_1 e^{-bkx} + A_2 e^{bkx}) \right] \cdot \exp[ik(y - ct)], \end{aligned} \quad (9a)$$

$$w' = A_5 e^{-b'kx} \cdot \exp[ik(y - ct)], \tag{9b}$$

where A_1, A_2, A_3, A_4 and A_5 are undetermined constants, $k (= 2\pi/\lambda, \lambda$ is the wavelength) is the wavenumber, $i^2 = -1$ and t is the time, c is the phase velocity of the Love wave. Equations (6) and (7) should be satisfied by Eqs. (9a) and (9b), then

$$b = ib_1 = i\sqrt{c^2/c_p^2 - 1}, \quad b' = \sqrt{1 - c^2/c_m^2} \tag{10}$$

The stress component and magnetic induction needed for the boundary and continuity conditions are [39]:

$$\sigma_{xz}(x, y, t) = [\bar{c}_{44}bk(-A_1e^{-bkx} + A_2e^{bkx}) + q_{15}k(-A_3e^{-kx} + A_4e^{kx})] \cdot \exp[ik(y - ct)], \tag{11a}$$

$$B_x(x, y, t) = -\mu_{11}k(-A_3e^{-kx} + A_4e^{kx}) \cdot \exp[ik(y - ct)], \tag{11b}$$

$$\sigma'_{xz}(x, y, t) = -c'_{44}b'kA_5e^{-b'kx} \cdot \exp[ik(y - ct)]. \tag{11c}$$

where $\bar{c}_{44} = c_{44} + q_{15}^2/\mu_{11}$ is the piezomagnetically stiffened elastic constant.

Equations (9a) and (9b) and (11a), (11b), (11c) are substituted into Eq. (8) to yields five linear homogeneous algebraic equations for five unknown coefficients A_1, A_2, A_3, A_4 and A_5 :

$$\begin{aligned} A_1 + A_2 &= A_5, \\ A_3 + A_4 + (A_1 + A_2)q_{15}/\mu_{11} &= 0, \\ \bar{c}_{44}b(A_2 - A_1) + q_{15}(A_4 - A_3) &= -c'_{44}b'A_5, \\ \bar{c}_{44}b(A_2e^{-bkh} - A_1e^{bkh}) + q_{15}(A_4e^{-kh} - A_3e^{kh}) &= 0, \\ -A_3e^{kh} + A_4e^{-kh} &= 0 \end{aligned} \tag{12}$$

To obtain the non-trivial solutions, the determinant of the coefficient matrix in Eq. (12) must be equal to zero, which yields the dispersion equation of Love waves propagation in the layered piezomagnetic structure

$$k_p^2 \tanh(2\pi H) + b_1 \tanh(b_1 2\pi H) - c'_{44}b'/\bar{c}_{44} = 0, \tag{13}$$

where $k_p^2 = q_{15}^2/\mu_{11}\bar{c}_{44}$ is the piezomagnetic coupling factor in the piezomagnetic layer, $H = h/\lambda$ is the dimensionless wavenumber.

From Eq. (12) the unknown constants A_1 – A_4 can be written in terms of A_5 as follows

$$A_1 = \frac{1}{1 + e^{2kbh}} A_5, \quad A_2 = \frac{e^{2kbh}}{1 + e^{2kbh}} A_5, \quad A_3 = \frac{-q_{15}/\mu_{11}}{1 + e^{2kh}} A_5, \quad A_4 = \frac{-q_{15}/\mu_{11}e^{2kh}}{1 + e^{2kh}} A_5 \tag{14}$$

Substituting Eq. (14) into Eq. (9a) and (9b), the mode shapes for displacement and magnetic potential in the thickness direction (the x -axis direction) of the piezomagnetic layer can be obtained as shown below

$$w(x, y, t) = A_5 \frac{e^{-kbx} + e^{kbx+2kbh}}{1 + e^{2kbh}} \exp[ik(y - ct)], \tag{15a}$$

$$\varphi(x, y, t) = A_5 \left(\frac{e^{-kbx} + e^{kbx+2kbh}}{1 + e^{2kbh}} - \frac{e^{-kx} + e^{kx+2kh}}{1 + e^{2kh}} \right) \cdot \frac{q_{15}}{\mu_{11}} \exp[ik(y - ct)] \tag{15b}$$

4 Numerical results and discussion

For the numerical calculation, Terfenol – D and metallic nickel are separately selected as the piezomagnetic layer and elastic substrate. The material constants used for calculation are summarized in Table 1 [40, 41]. A method to find the absolute minimum of the determinant of the coefficient matrix [42] is applied to solve the dispersion equation of the Love waves.

Table 1 Material constants of Terfenol-D [40] and Ni [41]

Terfenol-D		Ni			
ρ (kg/m ³)	9200	χ_m	20.4	ρ' (kg/m ³)	8905
E (GPa)	60	σ_s (MPa)	200	c'_{44} (GPa)	80
ν	0.3	$\mu_0 M_s$ (T)	0.96		
λ_s (ppm)	1950				

4.1 Effects of the magnetic field and compressive stress on the phase velocity of Love waves

Figure 2 shows the effect of the magnetic field H_z on the dispersion relation of Love waves propagation in the layered piezomagnetic structure when the compressive stress is $\sigma_z/\sigma_s = 0$. The vertical coordinate $c^* = c/c_m$ is the dimensionless phase velocity of a particular mode of the Love wave. The c_p and $c_{p'}$ in each figure are the bulk shear wave speeds under the different magnetic field H_z . For example: c_p and $c_{p'}$ in Fig. 2a are under $H_z = 0$ and 0.1 kOe respectively; c_p and $c_{p'}$ in Fig. 2b are under $H_z = 0.1$ and 1 kOe respectively; c_p and $c_{p'}$ in Fig. 2c are under $H_z = 1$ and 6 kOe respectively. The reason for choosing "Oersted" (Oe) not the SI unit (A/m) as the unit of the magnetic field strength is that a very large magnetic field strength should be applied on the magnetic material to reach the saturation magnetization state. So, "kOe" is adopted as the unit of the magnetic field strength is more convenient than "A/m" in the article (1Oe = 80 A/m, 1 kOe = 1000 Oe). As can be seen, the phase velocity of the Love waves c^* (first mode) decreases from the bulk shear wave speed in the substrate to that in the piezomagnetic layer. This is the typical phenomenon of Love waves propagation in a layered structure [37], and so the numerical results obtained in the article are verified to a certain extent. It is seen from Fig. 2a that the phase velocity c^* decreases as the magnetic field increases. This is because the piezomagnetically stiffened elastic constant \bar{c}_{44} decreases with an increasing magnetic field, which decreases the bulk shear wave speed in the piezomagnetic layer. As the magnetic field increases from 0.1 kOe to 1 kOe, the phase velocity c^* decreases greatly, and a new mode (The sixth mode) appears in the dispersion curves shown in Fig. 2b. As can be seen, the phase velocities c^* of the first five modes decrease obviously when the magnetic field increases from 0.1 kOe to 1 kOe. This phenomenon explains that a great change of the dispersion relation is caused by the small external magnetic field. As the magnetic field increases from 1 kOe to 6 kOe as shown in Fig. 2c, the phase velocity c^* decreases further. As seen in the Fig. 2, the propagation characteristics of Love waves can be improved substantially by increasing the magnetic field from 0.1 kOe to 6 kOe.

The effect of the compressive stress on the dispersion relation of Love waves at $H_z = 1$ kOe is shown in Fig. 3. The c_p , $c_{p'}$, and c_{p^*} are the bulk shear wave speeds in the piezomagnetic layer (at $H_z = 1$ kOe) under the compressive stress $\sigma_z/\sigma_s = 0$, $\sigma_z/\sigma_s = -0.1$, and $\sigma_z/\sigma_s = -0.5$, respectively. As can be seen from Fig. 3, the number of Love wave modes decrease as the compressive stress increases because the initial compressive stress makes the magnetic domain to rotate to the hard magnetization direction, i.e., the magnetic field strength is weakened by the compressive stress.

4.2 Effect of the magnetic field on the group velocity of Love waves

Figure 4 shows the phase velocity (c^*) and group velocity ($c_g^* = c^* + Hdc^*/dH$) of Love waves under different magnetic fields when the compressive stress is $\sigma_z/\sigma_s = 0$. As can be seen, the phase velocity c^* is always greater than the group velocity c_g^* of a Love wave mode. This illustrates that the phase velocity of a Love wave mode is always greater than the velocity of the mechanical energy carried by a particular mode. It should be noted that the starting point of the group velocity (the initial velocity of energy transport) of the high order mode is lower than that of the low order mode.

The effect of the magnetic field on the group velocity c_g^* of the Love waves at $\sigma_z/\sigma_s = 0$ is shown in Fig. 5. It is seen that the group velocity c_g^* decreases as the magnetic field increases at the same wavelength. In other words, the magnetic field can prevent the energy from radiating into the surrounding medium. Consequently, more energy is trapped in the piezomagnetic layer by applying the magnetic field. This result is extremely important for the application of SAW devices.

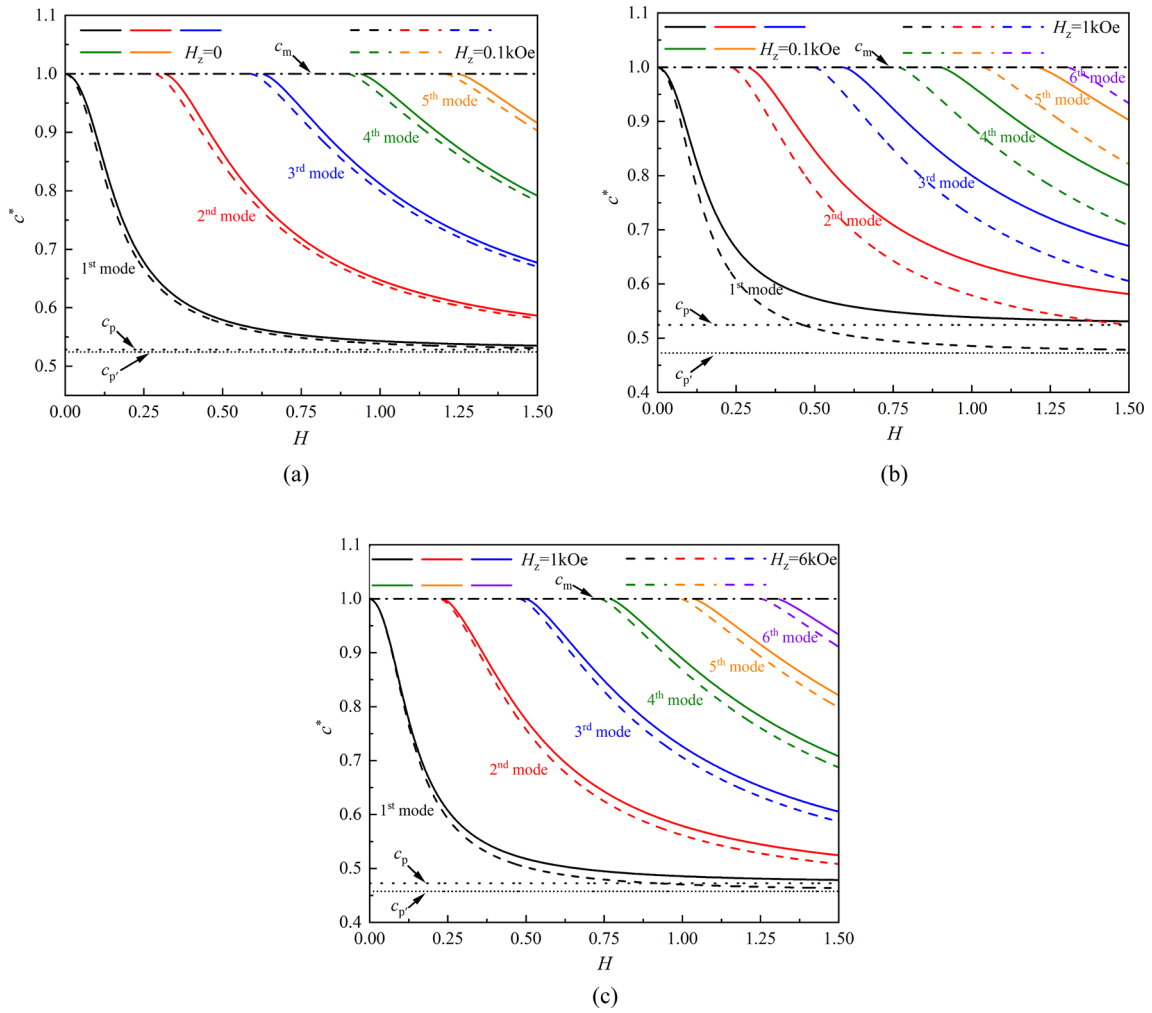


Fig. 2 Effect of the magnetic field on the dispersion relation of Love waves propagation in the layered piezomagnetic structure when the compressive stress is $\sigma_z/\sigma_s = 0$: **a** $H_z = 0$ and 0.1 kOe; **b** $H_z = 0.1$ and 1 kOe; **c** $H_z = 1$ and 6 kOe

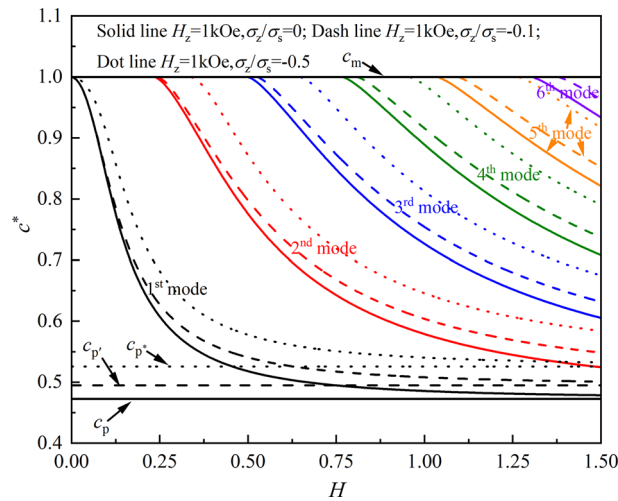


Fig. 3 Effect of the compressive stress on the dispersion relation of Love waves propagation in the layered piezomagnetic structure at $H_z = 1$ kOe

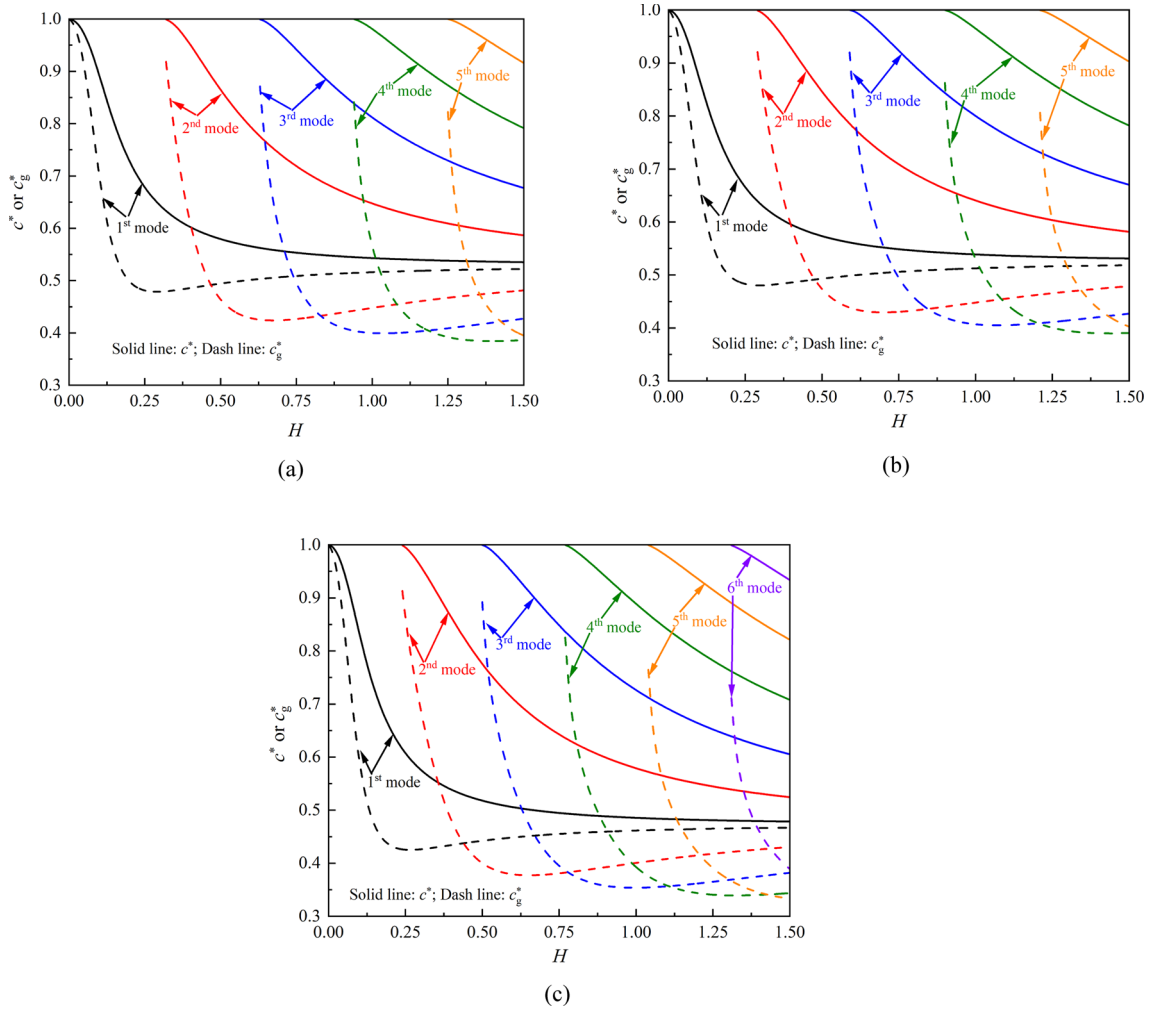


Fig. 4 Phase velocity (c^*) and group velocity (c_g^*) of Love waves under different magnetic fields when the compressive stress is $\sigma_z/\sigma_s = 0$: **a** $H_z = 0$; **b** $H_z = 0.1$ kOe; **c** $H_z = 1$ kOe;

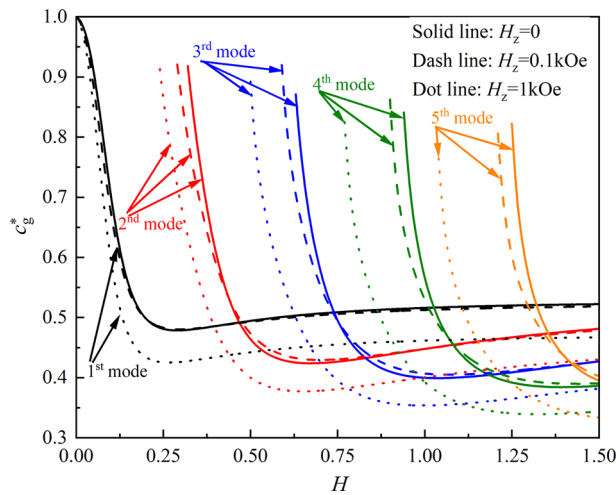


Fig. 5 Effect of the magnetic field on the group velocity c_g^* of the Love waves at $\sigma_z/\sigma_s = 0$

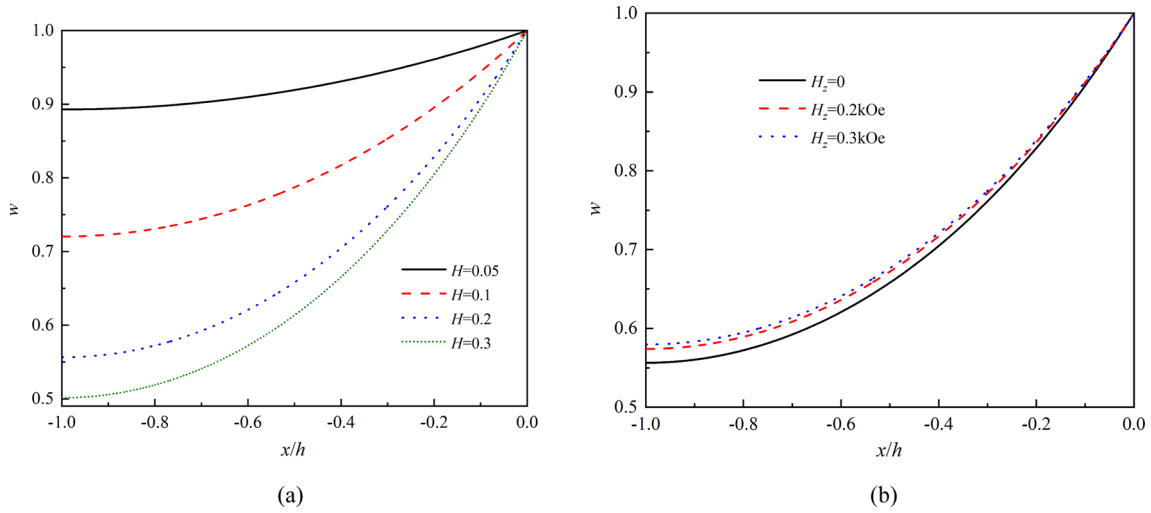


Fig. 6 Distribution of the displacement of the first order mode in the piezomagnetic layer, **a** for selected dimensionless wavenumber H at $H_z = 0$; **b** for selected magnetic field H_z at $H = 0.2$

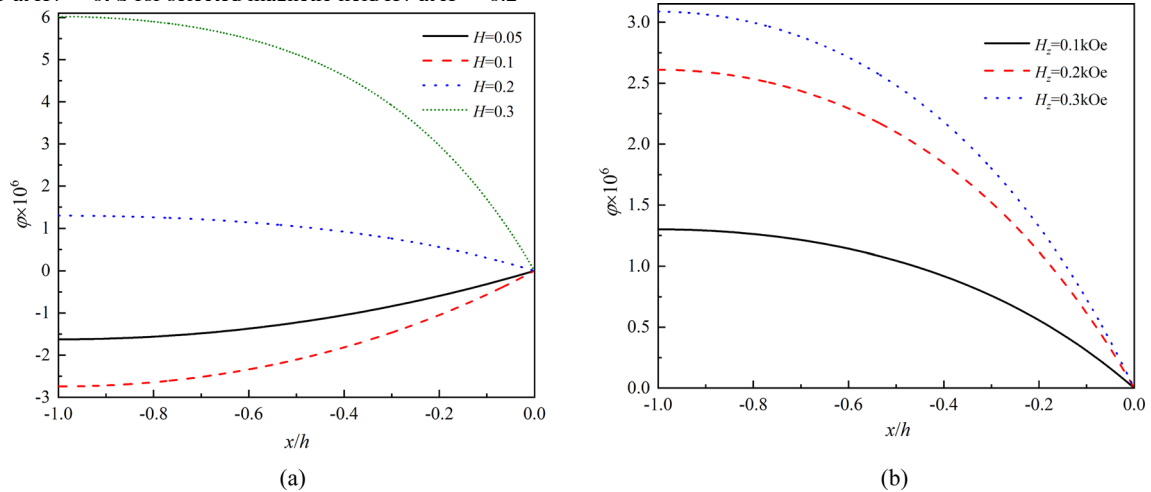


Fig. 7 Distribution of the magnetic potential of the first order mode in the piezomagnetic layer, **a** for selected dimensionless wavenumber H at $H_z = 0.1 \text{ kOe}$; **b** for selected magnetic field H_z at $H = 0.2$

4.3 Effect of the magnetic field on the mode shapes of the displacement and magnetic potential

The displacement w of the first order mode of Love waves in the piezomagnetic layer for selected dimensionless wavenumber H and magnetic field H_z is shown in Fig. 6. It can be seen from Fig. 6a that the displacement w increases from the layer surface to the interface between the layer and substrate. As the dimensionless wavenumber H increases, the displacement w decreases. Near the layer surface, there is a great difference among the displacements w at different wavenumbers H but this difference is reduced in the region near the interface. It can be seen from Fig. 6b that, as the magnetic field H_z increases from 0 to 0.2 kOe, the displacement increases significantly. There is no obvious change of the displacement w when the magnetic field H_z increases from 0.2 kOe to 0.3 kOe. As can be seen, the displacement w at the layer surface can be increased by the magnetic field H_z , this is desirable in the SAW devices with high performance.

The magnetic potential φ of the first order mode of Love waves in the piezomagnetic layer for selected dimensionless wavenumber H and magnetic field H_z is shown in Fig. 7. It is seen from Fig. 7a that the magnetic potential φ decreases firstly then increases with the dimensionless wavenumber H . The absolute value of the magnetic potential φ at the layer surface is maximum and this value equals to 0 at the interface between the layer and substrate. This is determined by the interfacial continuity conditions shown in Eq. (8c). The magnetic potential φ increases with the magnetic field H_z shown in Fig. 7b. The amplitude of the magnetic potential φ at the layer surface increases rapidly as the magnetic field H_z increases. The increase of the magnetic potential φ at the layer surface make the SAW devices suitable for designing sensors and transducers.

5 Conclusion

Effects of the magnetic field and compressive stress on propagation characteristics of Love waves in the layered piezomagnetic structure have been investigated theoretically in the article. The effective elastic, piezomagnetic and magnetic permeability constants in the piezomagnetic material are changed efficiently by the magnetic field and compressive stress. Numerical results show that the number of the modes increases as the magnetic field increase and the strength of the magnetic field is weakened by the compressive stress. As the magnetic field increases, the group velocity decreases but both the displacement and magnetic potential at the layer surface increase. The advantages of the method for tuning the propagation characteristics of Love waves proposed in the article are that the operation is easy and the device structure is not changed. The results obtained in the article are of great significance for designing high performance magneto-elastic SAW devices

Acknowledgements The National Natural Science Foundation of China (Nos. 11962015, 11872194 and 11862012) and the Natural Science Foundation of Shandong Province (No. ZR2020KA006) are gratefully acknowledged for their financial support.

Appendix 1

The matrix forms of Eq. (1)

The matrix forms of Eq. (1) are described as follows (using the engineering shear strain, i.e., $\gamma_{xy} = 2\varepsilon_{xy}$; $G = \frac{E}{2(1+\nu)}$):

$$\begin{aligned}
 \begin{Bmatrix} \varepsilon_x \\ \varepsilon_y \\ \varepsilon_z \\ \gamma_{yz} \\ \gamma_{zx} \\ \gamma_{xy} \end{Bmatrix} &= \begin{bmatrix} 1/E & -\nu/E & -\nu/E & 0 & 0 & 0 \\ -\nu/E & 1/E & -\nu/E & 0 & 0 & 0 \\ -\nu/E & -\nu/E & 1/E & 0 & 0 & 0 \\ 0 & 0 & 0 & 1/G & 0 & 0 \\ 0 & 0 & 0 & 0 & 1/G & 0 \\ 0 & 0 & 0 & 0 & 0 & 1/G \end{bmatrix} \begin{Bmatrix} \sigma_x \\ \sigma_y \\ \sigma_z \\ \tau_{yz} \\ \tau_{zx} \\ \tau_{xy} \end{Bmatrix} \\
 + \frac{\lambda_s}{M_s^2} &\begin{bmatrix} 1 - \tilde{\sigma}_x/\sigma_s & -1/2 - \tilde{\sigma}_x/\sigma_s & -1/2 - \tilde{\sigma}_x/\sigma_s & 0 & 0 & 0 \\ -1/2 - \tilde{\sigma}_y/\sigma_s & 1 - \tilde{\sigma}_y/\sigma_s & -1/2 - \tilde{\sigma}_y/\sigma_s & 0 & 0 & 0 \\ -1/2 - \tilde{\sigma}_z/\sigma_s & -1/2 - \tilde{\sigma}_z/\sigma_s & 1 - \tilde{\sigma}_z/\sigma_s & 0 & 0 & 0 \\ -2\tilde{\tau}_{yz}/\sigma_s & -2\tilde{\tau}_{yz}/\sigma_s & -2\tilde{\tau}_{yz}/\sigma_s & 3 & 0 & 0 \\ -2\tilde{\tau}_{zx}/\sigma_s & -2\tilde{\tau}_{zx}/\sigma_s & -2\tilde{\tau}_{zx}/\sigma_s & 0 & 3 & 0 \\ -2\tilde{\tau}_{xy}/\sigma_s & -2\tilde{\tau}_{xy}/\sigma_s & -2\tilde{\tau}_{xy}/\sigma_s & 0 & 0 & 3 \end{bmatrix} \begin{Bmatrix} M_x^2 \\ M_y^2 \\ M_z^2 \\ M_y M_z \\ M_z M_x \\ M_x M_y \end{Bmatrix}, \tag{A1}
 \end{aligned}$$

$$\begin{aligned} \begin{Bmatrix} H_x \\ H_y \\ H_z \end{Bmatrix} &= \frac{1}{kM} f^{-1} \left(\frac{M}{M_s} \right) \begin{bmatrix} 1 & 0 & 0 \\ 0 & 1 & 0 \\ 0 & 0 & 1 \end{bmatrix} \begin{Bmatrix} M_x \\ M_y \\ M_z \end{Bmatrix} \\ &- \frac{\lambda_s}{\mu_0 M_s^2} \begin{bmatrix} 2\tilde{\sigma}_x - \frac{I_\sigma^2 - 3I\sigma}{\sigma_s} & 2\tilde{\tau}_{xy} & 2\tilde{\tau}_{zx} \\ 2\tilde{\tau}_{xy} & 2\tilde{\sigma}_y - \frac{I_\sigma^2 - 3I\sigma}{\sigma_s} & 2\tilde{\tau}_{yz} \\ 2\tilde{\tau}_{zx} & 2\tilde{\tau}_{yz} & 2\tilde{\sigma}_z - \frac{I_\sigma^2 - 3I\sigma}{\sigma_s} \end{bmatrix} \begin{Bmatrix} M_x \\ M_y \\ M_z \end{Bmatrix}. \end{aligned} \quad (\text{A2})$$

Appendix 2

The effective material constants

The effective material constants of the piezomagnetic material can be expressed as follows:

$$\begin{aligned} c_{ijkl}(\mathbf{H}, \boldsymbol{\sigma}) &= S_{ijkl}^{-1}(\mathbf{H}, \boldsymbol{\sigma}), \\ q_{mij}(\mathbf{H}, \boldsymbol{\sigma}) &= c_{ijkl}(\mathbf{H}, \boldsymbol{\sigma}) \bar{q}_{mkl}(\mathbf{H}, \boldsymbol{\sigma}), \\ \mu_{nm}(\mathbf{H}, \boldsymbol{\sigma}) &= \bar{\mu}_{nm}(\mathbf{H}, \boldsymbol{\sigma}) - q_{nkl}(\mathbf{H}, \boldsymbol{\sigma}) S_{ijkl}(\mathbf{H}, \boldsymbol{\sigma}) q_{mij}(\mathbf{H}, \boldsymbol{\sigma}), \end{aligned} \quad (\text{B1})$$

where

$$S_{11} = \frac{1}{E} - \frac{\lambda_s M_z^2}{\sigma_s M_s^2} + \frac{k\lambda_s^2 \frac{M_z^2}{M_s^2} \left(1 + \frac{2\tilde{\sigma}_x}{\sigma_s}\right)^2}{\frac{\mu_0 M_s}{\frac{1}{M_3^2} - \csc^2(M_3)} - k\lambda_s \left(2\tilde{\sigma}_z - \frac{I_\sigma^2 - 3I\sigma}{\sigma_s}\right)}, \quad (\text{B2})$$

$$S_{12} = -\frac{\nu}{E} + \frac{\lambda_s M_z^2}{2\sigma_s M_s^2} + \frac{k\lambda_s^2 \frac{M_z^2}{M_s^2} \left(1 + \frac{2\tilde{\sigma}_x}{\sigma_s}\right) \left(1 + \frac{2\tilde{\sigma}_y}{\sigma_s}\right)}{\frac{\mu_0 M_s}{\frac{1}{M_3^2} - \csc^2(M_3)} - k\lambda_s \left(2\tilde{\sigma}_z - \frac{I_\sigma^2 - 3I\sigma}{\sigma_s}\right)}, \quad (\text{B3})$$

$$S_{13} = -\frac{\nu}{E} + \frac{\lambda_s M_z^2}{2\sigma_s M_s^2} - \frac{2k\lambda_s^2 \frac{M_z^2}{M_s^2} \left(1 + \frac{2\tilde{\sigma}_x}{\sigma_s}\right) \left(1 - \frac{\tilde{\sigma}_z}{\sigma_s}\right)}{\frac{\mu_0 M_s}{\frac{1}{M_3^2} - \csc^2(M_3)} - k\lambda_s \left(2\tilde{\sigma}_z - \frac{I_\sigma^2 - 3I\sigma}{\sigma_s}\right)}, \quad (\text{B4})$$

$$S_{22} = \frac{1}{E} - \frac{\lambda_s M_z^2}{\sigma_s M_s^2} + \frac{k\lambda_s^2 \frac{M_z^2}{M_s^2} \left(1 + \frac{2\tilde{\sigma}_y}{\sigma_s}\right)^2}{\frac{\mu_0 M_s}{\frac{1}{M_3^2} - \csc^2(M_3)} - k\lambda_s \left(2\tilde{\sigma}_z - \frac{I_\sigma^2 - 3I\sigma}{\sigma_s}\right)}, \quad (\text{B5})$$

$$S_{23} = -\frac{\nu}{E} + \frac{\lambda_s M_z^2}{2\sigma_s M_s^2} - \frac{2k\lambda_s^2 \frac{M_z^2}{M_s^2} \left(1 + \frac{2\tilde{\sigma}_y}{\sigma_s}\right) \left(1 - \frac{\tilde{\sigma}_z}{\sigma_s}\right)}{\frac{\mu_0 M_s}{\frac{1}{M_3^2} - \csc^2(M_3)} - k\lambda_s \left(2\tilde{\sigma}_z - \frac{I_\sigma^2 - 3I\sigma}{\sigma_s}\right)}, \quad (\text{B6})$$

$$S_{33} = \frac{1}{E} - \frac{\lambda_s M_z^2}{\sigma_s M_s^2} + \frac{4k\lambda_s^2 \frac{M_z^2}{M_s^2} \left(1 - \frac{\tilde{\sigma}_z}{\sigma_s}\right)^2}{\frac{\mu_0 M_s}{\frac{1}{M_3^2} - \csc^2(M_3)} - k\lambda_s \left(2\tilde{\sigma}_z - \frac{I_\sigma^2 - 3I\sigma}{\sigma_s}\right)}, \quad (\text{B7})$$

$$S_{44} = \frac{1}{G} - \frac{3\lambda_s M_z^2}{\sigma_s M_s^2} + \frac{9k\lambda_s^2 \frac{M_z^2}{M_s^2}}{3\mu_0 M_s - k\lambda_s \left(2\tilde{\sigma}_y - \frac{I_\sigma^2 - 3I\sigma}{\sigma_s}\right)}, \quad (\text{B8})$$

$$S_{55} = \frac{1}{G} - \frac{3\lambda_s M_z^2}{\sigma_s M_s^2} + \frac{9k\lambda_s^2 \frac{M_z^2}{M_s^2}}{3\mu_0 M_s - k\lambda_s \left(2\tilde{\sigma}_x - \frac{I_\sigma^2 - 3\Pi_\sigma}{\sigma_s}\right)}, \quad (\text{B9})$$

$$S_{66} = \frac{1}{G} - \frac{3\lambda_s M_z^2}{\sigma_s M_s^2}, \quad (\text{B10})$$

$$\bar{q}_{31} = -\frac{k\mu_0\lambda_s M_z \left(1 + \frac{2\tilde{\sigma}_x}{\sigma_s}\right)}{\frac{\mu_0 M_s}{\frac{1}{M_3^2} - \text{csc}^2 h^2(M_3)} - k\lambda_s \left(2\tilde{\sigma}_z - \frac{I_\sigma^2 - 3\Pi_\sigma}{\sigma_s}\right)}, \quad (\text{B11})$$

$$\bar{q}_{32} = -\frac{k\mu_0\lambda_s M_z \left(1 + \frac{2\tilde{\sigma}_y}{\sigma_s}\right)}{\frac{\mu_0 M_s}{\frac{1}{M_3^2} - \text{csc}^2 h^2(M_3)} - k\lambda_s \left(2\tilde{\sigma}_z - \frac{I_\sigma^2 - 3\Pi_\sigma}{\sigma_s}\right)}, \quad (\text{B12})$$

$$\bar{q}_{33} = \frac{2k\mu_0\lambda_s M_z \left(1 - \frac{\tilde{\sigma}_z}{\sigma_s}\right)}{\frac{\mu_0 M_s}{\frac{1}{M_3^2} - \text{csc}^2 h^2(M_3)} - k\lambda_s \left(2\tilde{\sigma}_z - \frac{I_\sigma^2 - 3\Pi_\sigma}{\sigma_s}\right)}, \quad (\text{B13})$$

$$\bar{q}_{24} = \frac{3k\mu_0\lambda_s M_z}{3\mu_0 M_s - k\lambda_s \left(2\tilde{\sigma}_y - \frac{I_\sigma^2 - 3\Pi_\sigma}{\sigma_s}\right)}, \quad (\text{B14})$$

$$\bar{q}_{15} = \frac{3k\mu_0\lambda_s M_z}{3\mu_0 M_s - k\lambda_s \left(2\tilde{\sigma}_x - \frac{I_\sigma^2 - 3\Pi_\sigma}{\sigma_s}\right)}, \quad (\text{B15})$$

$$\bar{\mu}_{11} = \mu_0 + \frac{k\mu_0^2 M_s^2}{3\mu_0 M_s - k\lambda_s \left(2\tilde{\sigma}_x - \frac{I_\sigma^2 - 3\Pi_\sigma}{\sigma_s}\right)}, \quad (\text{B16})$$

$$\bar{\mu}_{22} = \mu_0 + \frac{k\mu_0^2 M_s^2}{3\mu_0 M_s - k\lambda_s \left(2\tilde{\sigma}_y - \frac{I_\sigma^2 - 3\Pi_\sigma}{\sigma_s}\right)}, \quad (\text{B17})$$

$$\bar{\mu}_{33} = \mu_0 + \frac{k\mu_0^2 M_s^2}{\frac{\mu_0 M_s}{\frac{1}{M_3^2} - \text{csc}^2 h^2(M_3)} - k\lambda_s \left(2\tilde{\sigma}_z - \frac{I_\sigma^2 - 3\Pi_\sigma}{\sigma_s}\right)}, \quad (\text{B18})$$

with $M_z = M_s \left(\cot h M_3 - \frac{1}{M_3}\right)$ and $M_3 = kH_z + \frac{k\lambda_s M_z}{\mu_0 M_s^2} \left(2\tilde{\sigma}_z - \frac{I_\sigma^2 - 3\Pi_\sigma}{\sigma_s}\right)$.

References

1. Hashimoto, K.: *Surface Acoustic Wave Devices in Telecommunications*. Springer, Berlin (2000)
2. Love, A.E.H.: *Some Problems of Geodynamics*. Dover Publications Inc., New York (1967)
3. Bleustein, J.L.: A new surface wave in piezoelectric material. *Appl. Phys. Lett.* **13**(12), 412–413 (1968)
4. Yang, J.S.: Piezoelectric transformer structural modeling—a review. *IEEE Trans. Ultrason. Ferroelec.* **54**(6), 1154–1170 (2007)
5. Li, S.F.: The electromagneto-acoustic surface wave in a piezoelectric medium: the Bleustein–Gulyaev mode. *J. Appl. Phys.* **80**(9), 5264–5269 (1996)
6. Jin, F., Wang, Z.K., Wang, T.J.: The Bleustein–Gulyaev (B–G) wave in a piezoelectric layered half-space. *Int. J. Eng. Sci.* **39**(11), 1271–1285 (2001)
7. Li, P., Jin, F.: Bleustein–Gulyaev waves in a transversely isotropic piezoelectric layered structure with an imperfectly bonded interface. *Smart. Mater. Struct.* **21**(4), 045009 (2012)
8. Li, P., Jin, F., Qian, Z.H.: Propagation of the Bleustein–Gulyaev waves in a functionally graded transversely isotropic electro-magneto-elastic half-space. *Eur. J. Mech. A Solid.* **37**, 17–23 (2013)
9. Kayestha, P., Rodrigues Ferreira, E., Wijeyewickrema, A.C.: Finite-amplitude shear horizontal waves propagating in a pre-stressed layer between two half-spaces. *Int. J. Solids Struct.* **50**(22–23), 3586–3596 (2013)
10. Cao, X.S., Jin, F., Kishimoto, K.: Transverse shear surface wave in a functionally graded material infinite half space. *Philos. Mag. Lett.* **92**(5), 245–253 (2012)
11. Eskandari, M., Shodja, H.M.: Love waves propagation in functionally graded piezoelectric materials with quadratic variation. *J. Sound Vib.* **313**(1–2), 195–204 (2008)
12. Kielczynski, P., Szalewski, M., Balcerzak, A., Wieja, K.: Propagation of ultrasonic Love waves in nonhomogeneous elastic functionally graded materials. *Ultrasonics* **65**, 220–227 (2016)

13. Gulyaev, Y.V.: Review of shear surface acoustic waves in solids. *IEEE Trans. Ultrason. Ferroelectr.* **45**(4), 935–938 (1998)
14. Kielczynski, P., Pajewski, W.: Influence of a layered polarization of piezoelectric ceramics on shear-horizontal surface-wave propagation. *Appl. Phys. B Lasers O* **48**(5), 383–388 (1989)
15. Kielczynski, P., Pajewski, W., Szalewski, M.: Shear-horizontal surface waves on piezoelectric ceramics with depolarized surface layer. *IEEE Trans. Ultrason. Ferroelectr.* **36**(2), 287–293 (1989)
16. Kielczynski, P., Pajewski, W., Szalewski, M.: Shear horizontal surface waves on piezoelectric ceramic with layered structure. *Appl. Phys. A Mater.* **50**(3), 301–304 (1990)
17. Danoyan, Z.N., Piliposian, G.T.: Surface electro-elastic shear horizontal waves in a layered structure with a piezoelectric substrate and a hard dielectric layer. *Int. J. Solids Struct.* **45**(2), 431–441 (2008)
18. Du, J.K., Jin, X.Y., Wang, J., Xian, K.: Love wave propagation in functionally graded piezoelectric material layer. *Ultrasonics* **46**(1), 13–22 (2007)
19. Vashishth, A.K., Bareja, U.: Gradation and porosity's effect on Love waves in a composite structure of piezoelectric layers and functionally graded porous piezoelectric material. *Eur. J. Mech. A Solid* **99**, 104908 (2023)
20. Fan, H., Yang, J.S., Xu, L.M.: Antiplane piezoelectric surface waves over a ceramic half-space with an imperfectly bonded layer. *IEEE Trans. Ultrason. Ferroelectr.* **53**(9), 1695–1698 (2006)
21. Liu, J.X., Wang, Y.H., Wang, B.L.: Propagation of shear horizontal surface waves in a layered piezoelectric half-space with an imperfect interface. *IEEE T. Ultrason. Ferroelectr.* **57**(8), 1875–1879 (2010)
22. Li, P., Jin, F.: Excitation and propagation of shear horizontal waves in a piezoelectric layer imperfectly bonded to a metal or elastic substrate. *Acta Mech.* **226**(2), 267–284 (2015)
23. Su, J., Kuang, Z.B., Liu, H.: Love wave in ZnO/SiO₂/Si structure with initial stresses. *J. Sound Vib.* **286**(4–5), 981–999 (2005)
24. Qian, Z.H., Jin, F., Wang, Z.K., Kishimoto, K.: Love waves propagation in a piezoelectric layered structure with initial stresses. *Acta Mech.* **171**(1), 41–57 (2004)
25. Jin, F., Qian, Z.H., Wang, Z.K., Kishimoto, K.: Propagation behavior of Love waves in a piezoelectric layered structure with inhomogeneous initial stress. *Smart Mater. Struct.* **14**(4), 515–523 (2005)
26. Qian, Z.H., Jin, F., Kishimoto, K., Lu, T.J.: Propagation behavior of Love waves in a functionally graded half-space with initial stress. *Int. J. Solids Struct.* **46**(6), 1354–1361 (2009)
27. Du, J.K., Jin, J., Wang, J.: Love wave propagation in layered magneto-electro-elastic structures with initial stress. *Acta Mech.* **192**(1), 169–189 (2007)
28. Zhang, J., Shen, Y.P., Du, J.K.: The effect of inhomogeneous initial stress on Love wave propagation in layered magneto-electro-elastic structures. *Smart Mater. Struct.* **17**(2), 025026 (2008)
29. Liu, H., Kuang, Z.B., Cai, Z.M.: Propagation of Bleustein–Gulyaev waves in a prestressed layered piezoelectric structure. *Ultrasonics* **41**(5), 397–405 (2003)
30. Maerfeld, C., Gires, F., Tournois, P.: Bleustein–Gulyaev surface wave amplification in cds. *Appl. Phys. Lett.* **18**(7), 269–272 (1971)
31. Soluch, W.: Amplification of Bleustein–Gulyaev waves in tetragonal and hexagonal crystals. *J. Appl. Phys.* **45**(9), 3714–3715 (1974)
32. Soluch, W.: Theory of amplification of Bleustein–Gulyaev waves in tetragonal and hexagonal crystals. *IEEE Trans. Ultrason. Ferr.* **24**(1), 43–47 (1977)
33. Palanichamy, P., Singh, S.P.: Amplification of Bleustein–Gulyaev waves in cadmium sulfide. *J. Appl. Phys.* **54**(12), 6828–6833 (1983)
34. Gu, C.L., Jin, F.: Shear-horizontal surface waves in a half-space of piezoelectric semiconductors. *Phil. Mag. Lett.* **95**(2), 92–100 (2015)
35. Liu, X.E., Zheng, X.J.: A nonlinear constitutive model for magnetostrictive materials. *Acta Mech. Sin.* **21**(3), 278–285 (2005)
36. Gu, C.L., Jin, F.: Research on the tunability of point defect modes in a two-dimensional magneto-elastic phononic crystal. *J. Phys. D Appl. Phys.* **49**(17), 175103 (2016)
37. Liu, J.X., Fang, D.N., Wei, W.Y., Zhao, X.F.: Love waves in layered piezoelectric/piezomagnetic structures. *J. Sound Vib.* **315**(1–2), 146–156 (2009)
38. Curtis, R.G., Redwood, M.: Transverse surface waves on a piezoelectric material carrying a metal layer of finite thickness. *J. Appl. Phys.* **44**(5), 2002–2007 (1973)
39. Qian, Z.H., Jin, F., Hirose, S.: A novel type of transverse surface wave propagating in a layered structure consisting of a piezoelectric layer attached to an elastic half-space. *Acta Mech. Sin.* **26**(3), 417–423 (2010)
40. Gao, Y.W., Zhang, J.J.: Nonlinear magnetoelectric transient responses of a circular-shaped magnetoelectric layered structure. *Smart Mater. Struct.* **22**(1), 015015 (2013)
41. Auld, B.A.: *Acoustic Fields and Waves in Solids*. Wiley, New York (1973)
42. Zhu, F., Wang, B., Qian, Z.H.: A numerical algorithm to solve multivariate transcendental equation sets in complex domain and its application in wave dispersion curve characterization. *Acta Mech.* **230**(4), 1303–1321 (2019)

Publisher's Note Springer Nature remains neutral with regard to jurisdictional claims in published maps and institutional affiliations.

Springer Nature or its licensor (e.g. a society or other partner) holds exclusive rights to this article under a publishing agreement with the author(s) or other rightsholder(s); author self-archiving of the accepted manuscript version of this article is solely governed by the terms of such publishing agreement and applicable law.